ELSEVIER

Biophysical Chemistry 103 (2003) 271–288

Biophysical Chemistry

www.elsevier.com/locate/bpc

Comparison of the interaction, positioning, structure induction and membrane perturbation of cell-penetrating peptides and non-translocating variants with phospholipid vesicles

Mazin Magzoub, L.E. Göran Eriksson, Astrid Gräslund*

Department of Biochemistry and Biophysics, The Arrhenius Laboratories, Stockholm University, SE-106 91 Stockholm, Sweden

Received 30 April 2002; received in revised form 10 September 2002; accepted 16 September 2002

Abstract

Cell-penetrating peptides (CPPs) are able to translocate and carry cargo molecules across cell membranes. Using fluorescence techniques (polarization and quenching) and CD spectroscopy we studied the interaction, conformation and topology of two such peptides, transportan and 'penetratin' (pAntp), and two variants of differing translocating abilities, with small phospholipid vesicles of varying charge density. The induced structure of transportan is always helical independent of vesicle surface charge. pAntp and its two variants interact significantly only with negatively charged vesicles. The induced secondary structure depends on membrane charge and lipid/peptide ratio. The degree of membrane perturbation, evidenced by fluorescence polarization, of pAntp and its variants is related to their secondary structure. In the helical state, the peptides have little effect on the membrane. Under conditions where pAntp and its variants are converted into β-structures, they cause membrane perturbation. Oriented CD suggests that the two CPPs (pAntp and transportan) in their helical state lie along the vesicle surface, while the two pAntp variants appear to penetrate deeper into the membrane.

Keywords: Penetratin; Antennapedia; Transportan; Phospholipid vesicles; Structure induction; Translocation

Abbreviations: CPP, cell-penetrating peptide; pAntp, penetratin, Antennapedia homeodomain-derived CPP; W48F, variant of pAntp in which Trp48 has been replaced with a phenylalanine; 2W2F, non-translocating variant of pAntp in which both Trp48 and Trp56 have been replaced by phenylalanines; pIsl, Isl-1 homeodomain-derived CPP; Trp, tryptophan; CD, circular dichroism; OCD, oriented circular dichroism; POPC, 1-palmitoyl-2-oleoyl-phosphocholine; POPG, 1-palmitoyl-2-oleoyl-phosphoglycerol; 5- or 10-SLPC, 1-palmitoyl-2-(5- or 10-doxyl)stearoyl-*sn*-glycero-3-phosphocholine; DOPG, 1,2-dioleoyl-*sn*-glycero-3-phosphoglycerol; DPH, diphenylhexatriene, a membrane bound fluorescence probe; HFP, 1,1,1,3,3,3-hexafluoro-2-propanol; SUVs, small unilamellar vesicles; L/P, total phospholipid/peptide molar ratio.

*Corresponding author. Tel.: +46-8-162450; fax: +46-8-155597.
E-mail address: astrid@dbb.su.se (A. Gräslund).

0301-4622/03/$ - see front matter © 2002 Published by Elsevier Science B.V.
PII: S0301-4622(02)00321-6

1. Introduction

Cell-penetrating peptides (CPPs) are a new class of natural and synthetic water-soluble peptides, which are capable of translocating various cell membranes with high efficiency and low lytic activity. The mechanism is considered not to be endocytosis, and seems not to involve receptors or transporters [1,2]. The ability of the CPPs to translocate when covalently linked with a 'cargo', including polypeptides and oligonucleotides many times their own molecular mass, renders them of interest, both scientifically and biotechnologically. CPPs have so far been extensively used as vectors for the delivery of hydrophilic biomolecules and drugs into cytoplasmic and nuclear compartments of cells, both in vivo and in vitro [1,2].

The growing list of peptides classified as CPPs is large and varied. It includes so-called Tat-derived peptides, peptides based on signal sequences, as well as purely synthetic or chimeric peptides [1,2]. A large branch of the CPP family is composed of peptides with sequences derived from homeodomains of certain transcription factors. The first to be discovered of the homeodomain-derived translocating peptides is 'penetratin', which is also the most widely studied of the CPPs (Fig. 1). Penetratin, denoted pAntp, has a sequence corresponding to the 16 residues of the third α-helix (residues 43–58) of the Antennapedia homeodomain protein of *Drosophila* [3–5]. Residues 48 and 56 are tryptophans (Trp), which are useful fluorescent probes in pAntp. This third helix was found to be responsible for not only interaction with DNA by binding specifically to cognate sites in the genome [6], but also the translocation of the entire protein across cell membranes [5]. The pAntp peptide alone retains its membrane translocation properties and has therefore been proposed as a universal intercellular delivery vector [1]. The pIsl peptide (Fig. 1) is a newly discovered CPP from the homeodomain of another transcription factor (Isl-1), with a sequence homologous to pAntp, but with only one Trp residue, namely that corresponding to W48 in pAntp [7].

The mechanisms of translocation for the CPPs are still unknown. For instance, while it is clear that the peptide–membrane interactions must be of fundamental importance for the translocation process, it is as yet unclear what role, if any, the secondary structure plays in the translocation process, particularly since we have recently found

Peptide	Origin	Sequence	Translocation
pAntp (penetratin)	Antennapedia HD (homeotic family) residues 43-58	RQIKIWFQNRRMKWKK	yes
W48F	pAntp variant W48 replaced with F	RQIKIFFQNRRMKWKK	n.d.
2W2F	pAntp variant both W48 and W56 replaced with F	RQIKIFFQNRRMKFKK	no
pIsl	Isl-1 HD (LIM family) residues 45-60	RVIRVWFQNKRCKDKK	yes
Transportan	Chimera (galanin-mastoparan)	WTLNSAGYLLGKINLKALAALAKKIL	yes

Fig. 1. The origin, amino acid sequence and translocation ability of the peptides studied. The tryptophan (*bold W*) and charged residues (*underlined*) are highlighted.

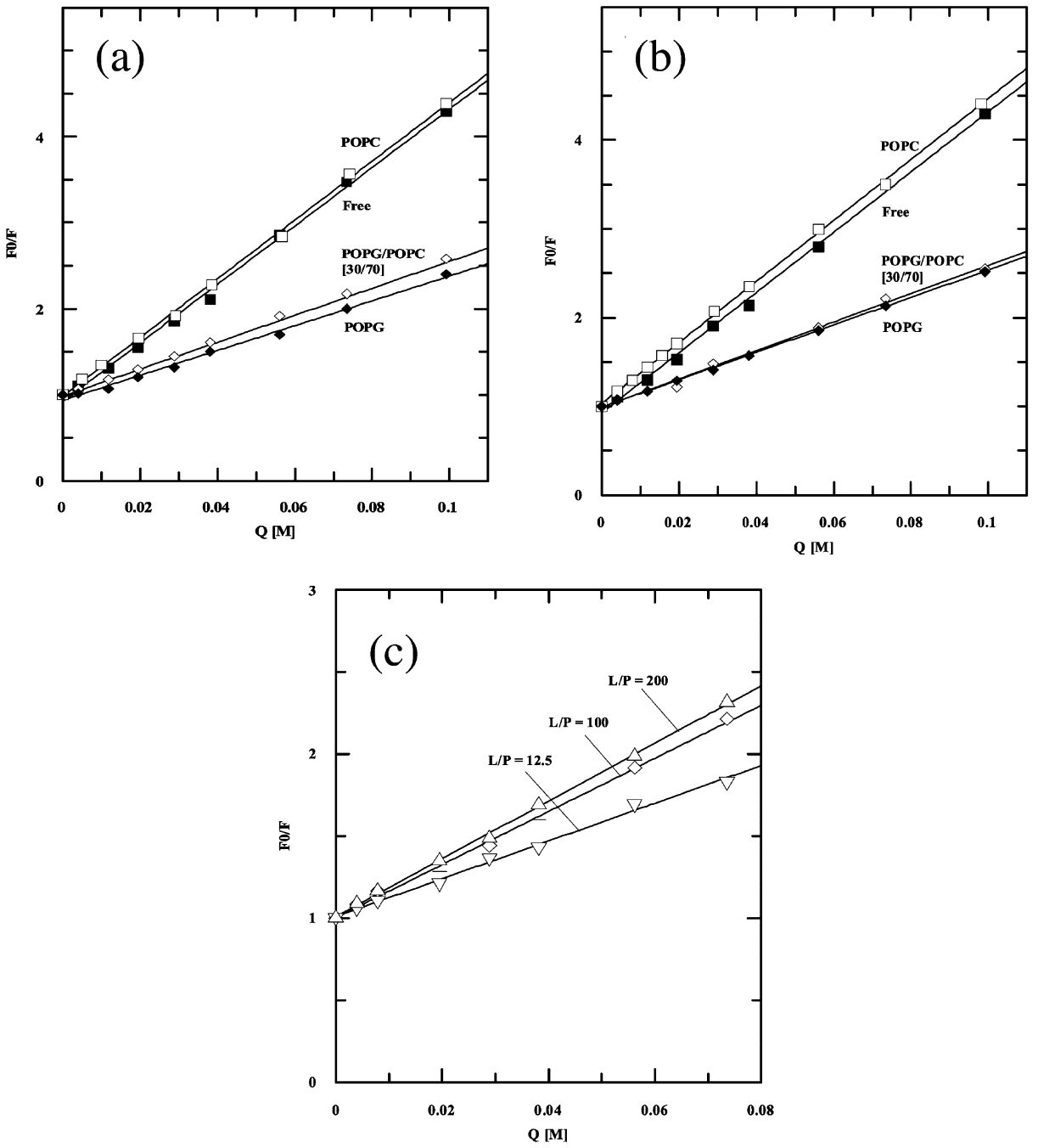

Fig. 2. Stern–Volmer plots for acrylamide quenching of the intrinsic Trp fluorescence of (a) pAntp and (b) W48F in the absence and presence of vesicles. Increasing concentrations of acrylamide, from a 1 M stock solution, were added to 10 μM of the peptide in the presence of either buffer or vesicles, composed of 1 mM phospholipid mixtures of different POPG/POPC content (L/P = 100). The samples contained buffer alone (■), and vesicles from POPC (□), POPG/POPC [30:70] (◇), or POPG (♦). The medium was 50 mM phosphate buffer (pH 7.0). (c) Stern–Volmer plots for acrylamide quenching of the Trp fluorescence of pAntp in 1 mM POPG/POPC [30:70] vesicles, at three different L/P ratios: 12.5 (▽), 100 (◇) and 200 (△). The medium was 50 mM phosphate buffer (pH 7.0). The spectra were recorded at ambient temperature (approx. 20 °C).

Table 1
Acrylamide quenching of the intrinsic tryptophan fluorescence of pAntp and its variant, W48F, with wavelength of the Trp fluorescence maximum, λ_{em}, and the Stern-Volmer constant, K_{SV}

Medium	L/P	pAntp		W48F	
		λ_{em} (nm)	K_{SV} (M^{-1})	λ_{em} (nm)	K_{SV} (M^{-1})
Buffer (pH 7)	–	354	35	354	35
POPC L/P	100	354	34	353	34
POPG L/P	100	338	14	339	15
POPG/POPC [30/70]	200	339	18	–	–
POPG/POPC [30/70]	100	339	16	339	16
POPG/POPC [30/70]	12.5	338	11	–	–

Measurements were made at an ambient temperature of approximately 20 °C. Peptide concentrations were 10 μM, in the presence of SUVs prepared from 1 mM phospholipids (L/P = 100), pH 7.0. The effect of the L/P ratio is also included for pAntp with POPG/POPC [30:70] vesicles.

that the induced secondary structure of pAntp is highly dependent on the environment [8,9].

The aim of the present study is to shed more light on any common characteristics of some CPPs upon membrane interactions. We have compared pAntp with 'transportan', another CPP with good vectorial properties (Fig. 1). Transportan is a chimeric fusion product between an N-terminal fragment from the galanin neuropeptide and the mastoparan peptide (wasp venom), with an extra lysine residue inserted between the two fused sequences [10]. We have also studied two variants of pAntp, denoted 2W2F and W48F, with different translocating abilities. The 2W2F variant, in which both Trp48 and Trp56 are replaced with phenylalanines, has been shown to have no significant translocating ability [3]. The W48F variant, in which the Trp48 has been replaced with phenylalanine, is expected to have reduced translocating ability [1,4]. Reduction in translocation has been reported for peptides where this Trp residue has been replaced by alanine [11,12]. The homologous pIsl peptide (Fig. 1), with an excellent translocating ability, has only one Trp residue, corresponding to Trp48 in pAntp.

We have used fluorescence techniques, including quenching with various types of quenchers, and static fluorescence polarization to study the interaction of the peptides with phospholipid vesicles of varying charge density. An estimate of the topology of the peptides in the vesicles was also obtained. Circular dichroism (CD) spectroscopy was used to characterize the corresponding secondary structures induced. Oriented CD spectroscopy (OCD) was also used to give information on the helical orientation of all the peptides when residing in the bilayer in their mainly helical state. The results show that the two CPPs, pAntp and transportan, lie close to the bilayer surface and with their helices preferentially perpendicular to the bilayer normal. The variants, W48F and 2W2F, on the other hand, appear to be inserted more parallel to the bilayer normal. These differences may be related to the varying translocation ability of the peptides.

2. Materials and methods

2.1. Materials

The peptides were produced by Neosystem Laboratoire, Strasbourg. The identity and purity were controlled by amino acid, mass spectral and HPLC analysis. The peptides were amidated in the N-terminus.

1-Palmitoyl-2-oleoyl-phosphatidylcholine (POPC), 1-palmitoyl-2-oleoyl-phosphatidylglycerol (POPG), and 1-palmitoyl-2-(5- or 10-doxyl)stearoyl-*sn*-glycero-3-phosphocholine (5- or 10-SLPC) were purchased from Avanti Polar Lipids, Alabaster, of the best quality, and used without further purification. Acrylamide was purchased from Kebo AB, Stockholm. DPH and the 5- and 12-doxyl stearic acids were from Sigma.

2.2. Preparation of vesicles

Vesicles were prepared by initially dissolving the phopholipids at the desired concentration (with the chosen POPG/POPC molar ratio) in chloroform to ensure complete mixing of the components, and then removing the solvent by placing the sample under high vacuum for 3 h. The dried lipids were then dispersed in 50 mM potassium phosphate buffer (pH 7.0). In some experiments the effect of the salt was also tested with the

presence of 150 mM potassium fluoride (KF) in the medium. For the topology experiments, phospholipids were mixed with the following molar ratio POPG/POPC/SLPC [30:60:10], i.e. with 10 mol.% of 5- or 10-SLPC, and 30% negative surface charge density (POPG). The ice-cooled dispersion was sonicated, using a Heat System model 350 A sonifier, under nitrogen until the transparency was maximized. The duration of sonication was approximately 30 min, with the microtip at a low output control (setting 4) and 50% duty cycle. Titanium particles and lipid debris were removed by centrifugation at $25\,000 \times g$. Ultracentrifugation was also used, but did not improve the light-scattering properties. This preparation procedure should result in vesicles of the small unilamellar type (SUVs), with dimensions of less than 100 nm in diameter [13].

2.3. Determination of peptide concentrations

After weighing on a microbalance, the peptide concentrations in the stock solutions were determined by light absorption on a CARY 4 spectrophotometer using cuvettes with a 2-mm light path. All the spectra were baseline-corrected. A molar absorptivity of 5600 M^{-1} cm^{-1} for one Trp residue was applied.

2.4. Fluorescence spectroscopy

Fluorescence was measured on a Perkin Elmer LS 50B luminescence spectrometer with FL WINLAB software. All measurements were made in 2×10-mm cuvettes at an ambient temperature of approximately 20 °C. For Trp fluorescence excitation was at 280 nm and the emission wavelength scanned from 300 to 500 nm. For DPH, fluorescence was excited at 340 nm and the emission scanned from 400 to 550 nm. Scans were recorded with 4-nm excitation and emission bandwidths and a scan speed of 250 nm min^{-1}. Three scans were recorded and averaged for each sample.

2.5. Acrylamide and spin-probe quenching

The concentration of peptides (P) was 10 μM, in the presence of SUVs from 1 mM phospholipids (L: POPC and/or POPG); L/P = 100. For the Trp fluorescence quenching experiments, acrylamide was added from an aqueous 1 M stock solution, resulting in concentrations between 4 and 100 mM. For samples containing vesicles, the background intensity was subtracted from the peptide-containing sample. Quenching constants K_{SV} were determined by a linear regression with the Stern–Volmer equation for a dynamic process [14]:

$$\frac{F_0}{F} = 1 + K_{SV}[Q] \quad (1)$$

where F and F_0 is the fluorescence intensity in the presence and the absence of acrylamide, respectively, and $[Q]$ is the total molar concentration of the quencher in the sample.

The ability of spin-labels to act as a fluorescence quencher was also employed to give information on the accessibility of the tryptophans within the lipid bilayer. A 20 μM concentration of the peptides was added to vesicles composed of 2 mM phospholipid mixture of different POPG/POPC content. Either 5-doxyl or 12-doxyl stearic acid was added from a 5 mM ethanolic stock solution, resulting in concentrations between 25 and 200 μM of the spin label. After allowing the system to equilibrate, the intrinsic Trp fluorescence of the peptide was measured. The quenching constants K_{SV} were again determined by a linear regression with the Stern–Volmer equation [Eq. (1)]. By the degree of quenching that has taken place, it is also possible to judge the proximity of the Trp residue of the peptide relative to the spin label at the 5- and 12-doxyl positions. However, for that purpose we employed spin-labeled phosphatidylcholines (SLPC) instead of the free fatty acids (vide infra).

2.6. Determination of the topology of the peptides in vesicles

To estimate the distance of the Trp residues from the center of the bilayer, the peptides were added to vesicles composed of POPG/POPC [30:70] (i.e. with 30% surface charge density), with or without 10 mol.% 5- or 10-SLPC, at an L/P of 100. The distances of the Trp residues of the peptides from the center of the bilayer were then calculated using the parallax equation [15,16]:

$$Z = L_1 + \frac{\left(-\ln(F_1/F_2)/\pi C - L_2^2\right)}{2L_2} \quad (2)$$

where Z is the average distance of the fluorophore from the center of the bilayer, F_1 is the relative fluorescence ratio (F/F_0) reduction due to the shallow quencher (5-doxyl), F_2 is the fluorescence ratio of the deeper quencher (10-doxyl), L_1 is the distance of the shallow quencher from the center of the bilayer, L_2 is the distance between the two quenchers and C is the average surface concentration of the quencher (SLPC) in molecules $Å^{-2}$, or mole fraction of SLPC/70 $Å^2$ [15]. The cross-section of a phosphatidylcholine (PC) headgroup was assumed to be approximately 70 $Å^2$, resulting in a SLPC surface concentration of $0.1/70 = 1.4\times10^{-3}$ $Å^{-2}$ in the present case. The values used for the distances of the two spin-label groups from the center of the bilayer (L_1) were 7.7 and 12.2 Å for 10- and 5-doxyl, respectively [15,16]. Hence, $L_2 = 4.5$ Å.

2.7. Fluorescence polarization

Labeling the vesicles with the membrane-bound probe DPH, we monitored the membrane perturbation upon addition of the peptides. To prepare the samples, 2 μM DPH (from a 1 mM ethanolic stock solution) was added to SUVs composed of 1 mM phospholipid mixtures of different POPG/POPC content. The samples were allowed to stand for 10 min before measurement. Increasing concentrations of peptides, from a 1 mM stock solution, were added to the samples. A polarization attachment (Shimadzu) was adapted to the spectrometer. The steady-state polarization was determined using the following equation [14]:

$$P = \frac{I_{VV} - GI_{VH}}{I_{VV} + GI_{VH}} \quad (3)$$

where I_{VV} is the emission intensity of vertically polarized light parallel to the plane of excitation and I_{VH} is the emission intensity of horizontally polarized light perpendicular to the plane of excitation. The instrumental factor G ($G = I_{HV}/I_{HH}$) was determined by measuring the polarized components of fluorescence of the probe with horizontally polarized excitation.

2.8. Circular dichroism spectroscopy

CD measurements were made on a Jasco J-720 CD spectropolarimeter with 0.5- and 1-mm quartz cuvettes. Spectra were measured from 190 to 250 nm, with 0.2-nm step resolution at 100-nm min^{-1} scan speed. The response time was 4 s, with 50 mdeg sensitivity and 2-nm bandwidth. The temperature was regulated with a PTC-343 controller set at 20 °C. Spectra were collected and averaged over 40 scans. Contributions from background signals were subtracted from the CD spectra acquired for the peptide. Computer fittings using the VARSELEC program [17] were performed to estimate the contributions of spectral components from different secondary structures. For a short, flexible peptide, these estimations should not be taken as exact evaluations of secondary structure contribution, but rather reflecting relative changes under varying conditions.

2.9. Oriented circular dichroism

OCD measurements were made on a Jasco J-720 CD spectropolarimeter, with a standard cylindrical cuvette of 2 cm in diameter. The spectra were measured by use of oriented multibilayers, following the procedures of Huang and co-workers [18–20]. Peptide and lipid were co-dissolved in methanol at 40 μM and 14 mM, respectively. Approximately 40 μl of this stock solution (with L/P = 100) was carefully layered onto one of the cylindrical cuvette surfaces. Solvent was removed under a stream of nitrogen, followed by hydration of the samples by placing a drop of water at the bottom of the cuvette before sealing. The cuvette was then placed in a holder in the spectrometer, with the sample surface perpendicular to the optical axis. The background signal correction was determined with the same amount of lipid, but without peptide, and subtracted.

3. Results

3.1. Acrylamide fluorescence quenching

The intrinsic Trp fluorescence of pAntp and its variant W48F (sequences in Fig. 1) was studied

in various solvent media, including small, unilamellar phospholipid vesicles with varying negative charge. pAntp has two Trp residues, (Trp48 and Trp56) whereas W48F has only one (Trp56). The Trp fluorescence from both peptides obeys the linear Stern–Volmer equation with acrylamide as a neutral hydrophilic quencher.

In aqueous buffer alone, pAntp has an overall wavelength of Trp fluorescence maximum (λ_{em}) of 354 nm, and a Stern–Volmer quenching constant (K_{SV}) of 35 M^{-1} (Fig. 2a and Table 1), identical to the values measured for monomeric (free) Trp itself in buffer [8]. In the presence of neutral POPC vesicles, pAntp has approximately the same values as in buffer, and therefore does not appear to associate to the vesicles, in agreement with our earlier study [8]. In the presence of negatively charged POPG containing vesicles, the peptide behaves in the same manner at both 30% and 100% surface charge density, with λ_{em} being shifted to approximately 338 nm, accompanied by increased fluorescence intensity.[1] This shift towards a shorter wavelength ('blue shift') is representative of the Trp residues being partitioned into a more hydrophobic environment [14]. This also indicates that the Trp residues are only partially buried in the vesicles, even at the higher lipid charge density, since a moiety fully protected from water is expected to have emission at approximately 320 nm [14]. Partial protection from the aqueous solvent is further supported by the corresponding decrease in the K_{SV} value to 16 M^{-1} in POPG/POPC [30:70] vesicles, and 14 M^{-1} in 100% POPG vesicles. These values also suggest that the Trp residues are slightly better protected from the quencher with the fully charged vesicles. There is no indication from the Stern–Volmer graphs that the two Trp residues in pAntp (W in Fig. 1) respond differently to the quenching.

The behavior of pAntp is mirrored by its variant W48F, with its single Trp56 (Fig. 2b). In buffer, W48F has λ_{em} of approximately 354 nm and K_{SV} of 35 M^{-1} (Table 1). In the presence of neutral POPC vesicles there is no wavelength shift and therefore, again, no evidence for binding. With 30% and 100% charged vesicles, λ_{em} is blue-shifted to approximately 339 nm and K_{SV} is reduced to approximately 16 and 15 M^{-1}, respectively. This means that both pAntp and W48F interact similarly with vesicles, and that the membrane association is charge-dependent. From the acrylamide quenching it is clear that the fluorophores of the two peptides reside in approximately the same region, since there is no significant distinction between the two Trp residues of pAntp and the single Trp of W48F. Accordingly, we previously observed similar values of λ_{em} and K_{SV} for the single Trp of DOPG-bound pIsl (corresponding to W48 in pAntp) [8].

The acrylamide quenching properties of pAntp bound to POPG/POPC [30:70] vesicles, in the L/P range 12.5–200, are shown in Fig. 2c and Table 1. A low L/P condition makes the fluorophores less accessible to the quencher. We have observed [9] that the different L/P ratios give rise to different secondary structural states of bound pAntp: at high L/P, pAntp adopts a dominating helical conformation, while at low L/P it adopts mostly a β-structure, possibly as a result of β-sheet aggregation. The different secondary structures may be correlated with varying exposure to the quencher, i.e. at the low L/P with a dominating β-structure, the Trp moieties are more hidden from the quencher.

3.2. Fatty acid spin-probe fluorescence quenching

To obtain more information about the location of pAntp, W48F and transportan within the vesi-

[1] While this manuscript was under review, a study was published on the interaction of pAntp with vesicles comprised of mixtures of neutral egg yolk phosphatidylcholine and negatively charged bovine brain phosphatidylserine [B. Christiaens, S. Symoens, S. Vanderheyden, Y. Engelborghs, A. Joliot, A. Prochiantz, J. Vandekerckhove, M. Rosseneu, B. Vanloo, Tryptophan fluorescence study of the interaction of penetratin peptides with model membranes, Eur. J. Biochem. 269 (2002) 2918–2926.]. The authors observed that the binding of the peptide to the vesicles was accompanied by a decrease in the fluorescence intensity, and suggested various explanations for this. In view of our present observation of increased fluorescence intensity of pAntp interacting with POPC/POPG mixed vesicles, we would support the suggested explanation of specific quenching of Trp fluorescence by the serine headgroups, rather than internal peptide quenching. This explanation is also supported by our observation of pAntp fluorescence quenching by free serine in aqueous solution (data not shown).

cles, spin-labeled fatty acid probes (5- and 12-doxyl stearic acid) were used to quench the intrinsic Trp fluorescence of the peptides from the inside of the bilayer (Fig. 3a,b). 5-Doxyl stearic acid has its fluorescence-quenching paramagnetic doxyl group close to the surface of the bilayer, whereas 12-doxyl stearic acid has its doxyl group buried more deeply in the bilayer [15,16]. Table 2 gives the Stern–Volmer quenching constant (K_{SV}) derived for both quenchers with two different vesicles preparations, with L/P = 100. Even with this type of quencher, linear Stern–Volmer relationships are obtained for the peptides.

For all three peptides, the shallow 5-doxyl probe quenches the Trp fluorescence more effectively than the deeper 12-doxyl probe. This indicates that Trp moieties of these peptides should reside near the surface of the bilayer, i.e. close to the headgroups. As also suggested by the acrylamide

Table 2
Stern–Volmer constant K_{SV} for quenching of the intrinsic Trp fluorescence of the transportan, pAntp, and W48F peptides by spin-labeled fatty acids

Medium	Peptide	K_{SV} (M^{-1})	
		5-Doxyl stearic acid	12-Doxyl stearic acid
POPG/POPC [30:70]	pAntp	8.2	2.2
	W48F	7.4	1.7
	Transportan	5.2	0.8
POPG	pAntp	5.1	1.0
	W48F	5.3	0.5
	Transportan	4.8	0.9

An ambient temperature of approximately 20 °C was employed. Peptide concentrations were 20 μM in the presence of SUVs prepared from 2 mM phospholipids (L/P = 100), pH 7.0.

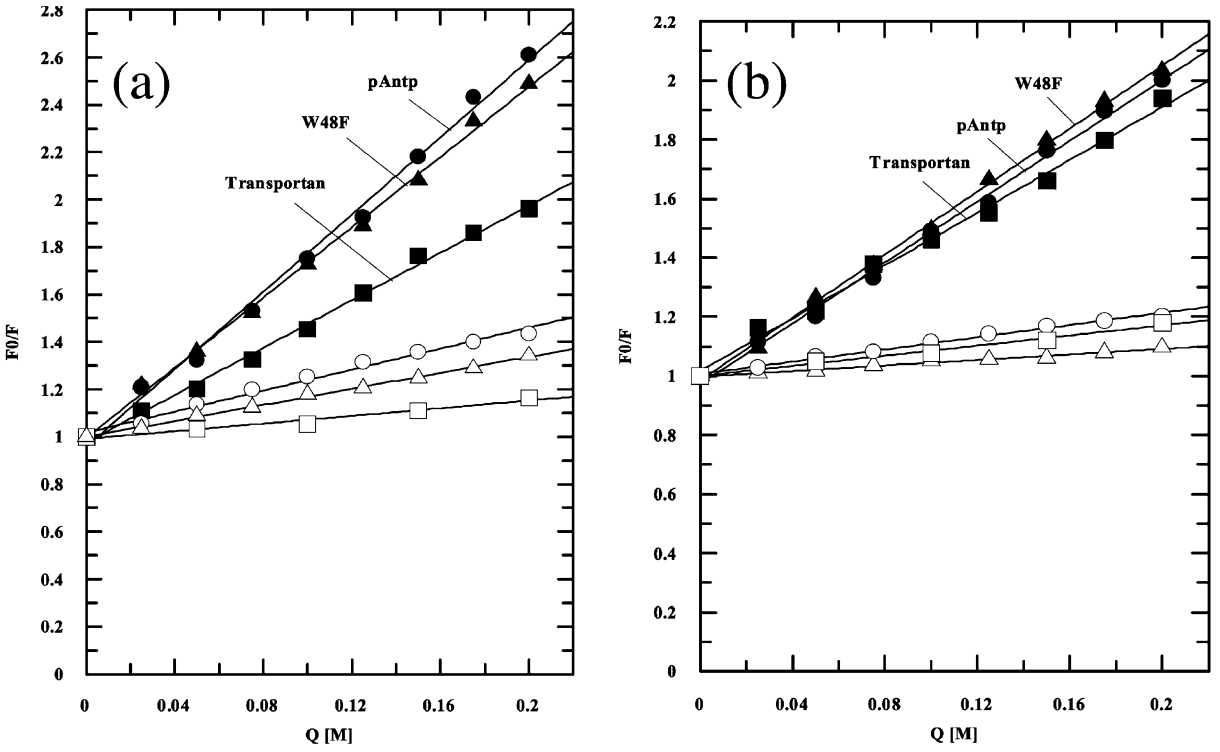

Fig. 3. Stern–Volmer plots of the spin-labeled stearic acid quenching of the intrinsic Trp fluorescence of transportan (■), pAntp (●), and W48F (▲) in the presence of SUVs composed of 2 mM of (a) POPG/POPC [30:70], or (b) POPG. The L/P ratio was 100. Increasing concentrations of 5-doxyl (*filled symbols*) or 12-doxyl (*open symbols*) stearic acid were incorporated into the vesicles. The medium was 50 mM phosphate buffer (pH 7.0). The spectra were recorded at ambient temperature (approx. 20 °C).

Table 3
Estimation by the parallax method [15,16] of the depth of the Trp residues of transportan, pAntp and its variant W48F, and pIsl in SUVs

Peptide	F_1	F_2	Z (Å)
pAntp	0.75	0.85	13.0
W48F	0.79	0.96	14.5
Transportan	0.80	0.89	12.5
pIsl	0.78	0.86	12.3

The phospholipid vesicles were prepared from POPG/POPC/5- or 10-SLPC [30:60:10] (L/P = 100). Given in the table are F_1, the relative fluorescence ratio (F/F_0) reduction due to the shallow quencher (5-doxyl), and F_2 the fluorescence ratio of the deeper quencher (10-doxyl). The average distance of the Trp from the center of the bilayer (Z) was calculated [with Eq. (2)] for a 5- or 10-SLPC concentration of 10 mol.%, with $L_1 = 12.2$ Å (the distance of the shallow quencher from the center of the bilayer) and $L_2 = 4.5$ Å (the distance between the two quenchers). The Z-value is the average of three readings. The relative uncertainty (estimated by comparison of results from repeated experiments) is approximately ± 0.5 Å.

quenching results, the two Trp residues of pAntp reside in the same region.

Interestingly, the quenching constants for the pAntp and its variant are lower for the 100% POPG vesicles, compared to vesicles with only 30% POPG, at the same L/P ratio of 100 (Table 2). This is in agreement with the acrylamide quenching results, which indicate that at the higher lipid charge density, the two Trp residues are hidden further from the quenchers, possibly related to aggregation of the peptide in a β-structure state.

3.3. Determination of the topology of the peptides in vesicles

For vesicles containing 10 mol.% of 5- or 10-SLPC at a 30% surface charge density (POPG/POPC/SLPC [30:60:10]) and an L/P value of 100, the distances of the Trp residues of the peptides from the center of the bilayer were estimated using the parallax method [15,16]. Table 3 shows the positions obtained by Eq. (2) for the Trp residues of transportan, pAntp, W48F and pIsl. The relative uncertainty (estimated by comparison of results from repeated experiments) is of the order of ± 0.5 Å. Taking the average length of the acyl chains of the membrane bilayer to be 15 Å [15], the results show that the Trp residues of all three peptides are located below the membrane head groups. The average position for the two Trp residues of pAntp is at 13.0 Å from the bilayer center. The single Trp of the pIsl CPP (Fig. 1) is calculated to be somewhat more deeply inserted into the bilayer than the single W56 of the W48F peptide.

3.4. Fluorescence polarization

The effect of pAntp, its variants and transportan on the membrane order and dynamics ('fluidity') was studied by fluorescence polarization. Vesicles with varying charge density were labeled with DPH as a membrane fluorescence probe. Upon addition to a membrane suspension, DPH dissolves completely in the bilayer core, with no significant emission from the probe in the aqueous environment [14]. The polarization of the probe upon the addition of increasing concentrations of the peptides to phospholipid vesicles (1 mM) was measured. When a change was observed it was linearly dependent on the peptide concentration, with L/P ≥ 10.

Fig. 4a shows the polarization effect of transportan and the pAntp peptides on neutral POPC vesicles. pAntp and its variants do not affect the DPH polarization significantly, confirming that no interaction of pAntp takes place with neutral vesicles [8]. This is also supported by the quenching results (Fig. 2a).

Fig. 4b shows the effect of the peptides on POPG/POPC [30:70] vesicles. pAntp again induces no significant change in the DPH fluorescence polarization. This means that although pAntp does interact with the vesicles with 30% surface charge [9], in contrast to the case of neutral POPC, it does not appear to perturb the membranes to a great extent. With the two pAntp variants, a slight increase in the polarization is observed, probably due to the higher hydrophobicity of the peptides, with the effect being more prominent with the 2W2F variant than with W48F.

With 1 mM POPG vesicles, pAntp and its variants cause a considerable increase in the DPH polarization (Fig. 4c), suggesting significant membrane perturbation at the very high surface-

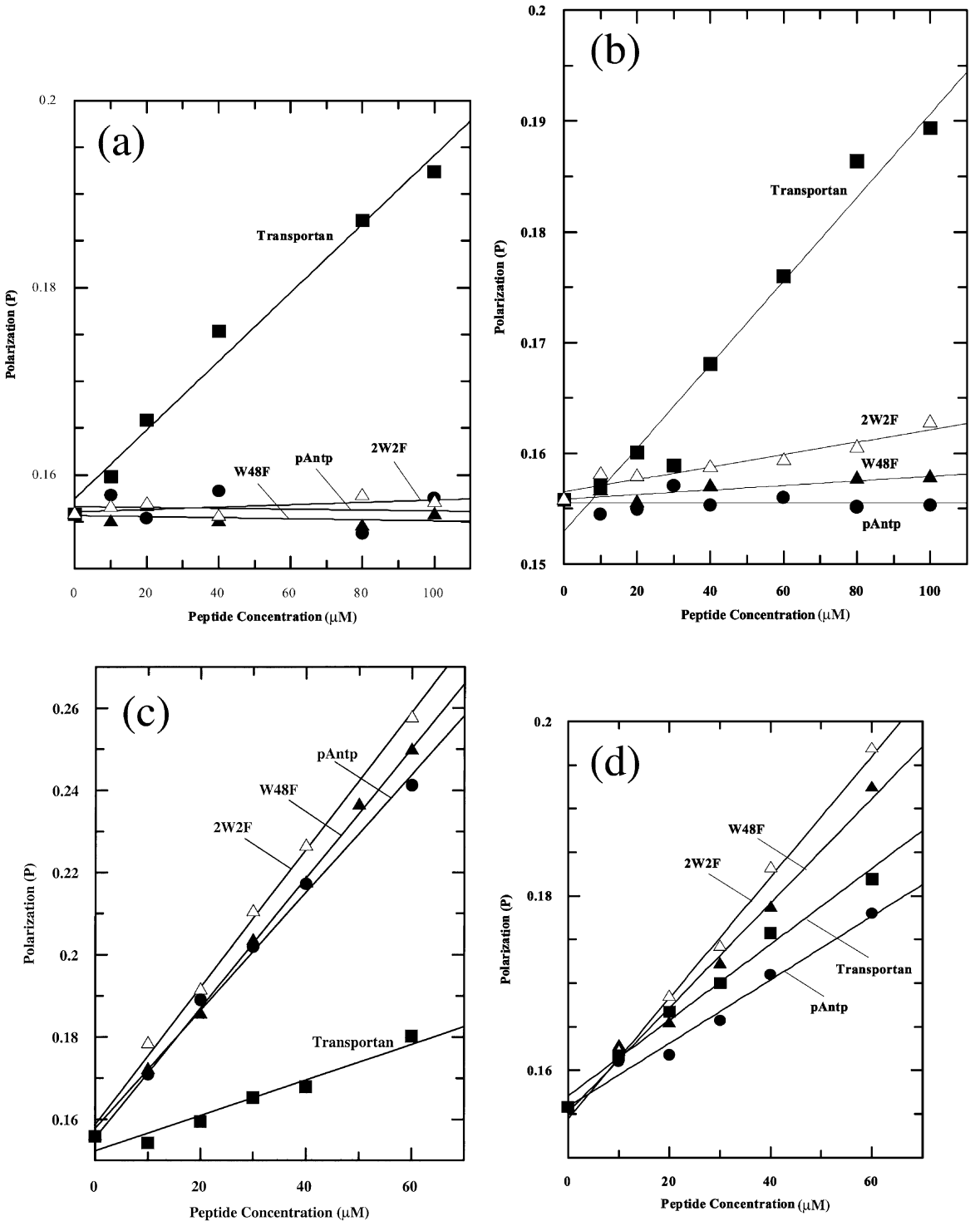
(a)
Transportan
pAntp
2W2F
W48F
Polarization (P)
Peptide Concentration (μM)
(b)
Transportan
2W2F
W48F
pAntp
Polarization (P)
Peptide Concentration (μM)
(c)
pAntp
W48F
2W2F
Transportan
Polarization (P)
Peptide Concentration (μM)
(d)
W48F
2W2F
Transportan
pAntp
Polarization (P)
Peptide Concentration (μM)

Fig. 4.

charge density. Reducing the effect of electrostatics by adding salt (150 mM KF) results in a reduced effect on the DPH polarization (Fig. 4d).

Transportan, on the other hand, causes the same degree of increase in DPH polarization, regardless of the membrane charge density. Transportan, with its highly hydrophobic mastoparan C-terminus, does not require a charged membrane in order to interact [8], and its stabilized helical structure is insensitive to the charge density (vide infra).

3.5. Circular dichroism spectroscopy

The structure induced in pAntp and its two variants, as well as transportan, in the presence of vesicles of different compositions was studied by CD spectroscopy. Fig. 5a shows the CD spectra of the peptides in buffer alone (pH 7). The varying components of secondary structures were evaluated by computer fitting to sums of pure α, β and random-coil component spectra [17]. Transportan is largely unstructured with a small α-helix contribution (approx. 30%). pAntp and its two variants are mostly unstructured (random coil), although some β-structure contribution exists.

Fig. 5b shows the CD spectra of the peptides in the presence of 1 mM POPG/POPC [30:70] vesicles, with L/P = 100. Transportan adopts a mainly α-helical conformation (approx. 60%), as does pAntp, but with a somewhat lesser helicity (55%). The two variants are even less helical. TheW48F variant has approximately 40% α-helix. The 2W2F variant has only 25% helix, and the remaining components are 60% random coil and 15% β-structure. However, in aqueous 30% HFP solvent the 2W2F and W48F variants both show a high degree of helicity (data not shown), comparable to that of pAntp.

Fig. 5c includes the CD spectra of the peptides in the presence of 1 mM POPG vesicles at L/P = 100. pAntp and its variants now adopt predominantly β-structures, with 2W2F giving the highest percentage (55%), followed by W48F (50%) and pAntp (45%). In the presence of 1 mM POPG vesicles with 150 mM KF added to the medium (Fig. 5d), pAntp and its variants revert to a more helical state. Transportan adopts a helical structure in the presence and absence of salt, with the same degree of helicity induced in pure POPG vesicles as with POPG/POPC [30:70] vesicles, indicating that no lipid charge-dependent structural conversion of the peptide takes place (Fig. 5c,d).

CD studies of transportan at L/P ratios varying between 12.5 and 100, with 100% POPG vesicles, gave no conclusive evidence of an L/P-dependent α → β structure conversion, although the helicity was somewhat lower at the lowest L/P ratio (data not shown). This is contrast to the strong structural L/P dependence of the observed α → β structure conversion with pAntp [9].

3.6. Oriented circular dichroism

Fig. 6 shows the OCD spectra of the peptides in oriented POPG/POPC [30:70] multibilayers, where the peptides should have a variable degree of helical structure (cf. Fig. 5b). The spectrum for pAntp has the characteristic shape and extreme positions expected for a peptide α-helix lying along the surface, i.e. perpendicular to the bilayer normal [18–21]. The spectrum for transportan also resembles that of a surface helix. The spectra for the two pAntp variants, W48F and 2W2F, are quite different. They may show effects of aggregation, but are also quite similar to the spectrum of a helix oriented perpendicular to the membrane [20,21], suggesting that the helical moieties of the variants might insert more parallel to the bilayer normal. The insert in Fig. 6 shows the spectra of helices in the two extreme orientations, after Wu et al. [20]. However, the low inherent helicity of the variants (in particular 2W2F) in the presence of vesicles with 30% charge density (Fig. 5b) makes the analysis complicated, since the OCD

Fig. 4. Fluorescence polarization (*P*) of DPH-labeled vesicles as a function of peptide concentration. Increasing concentrations of the peptides—transportan (■), pAntp (●), W48F (▲) and 2W2F (△)—were added to SUVs composed of 1 mM phospholipid samples of different POPG/POPC content, and containing 2 μM DPH. The sample contained: (a) POPC; (b) POPG/POPC [30:70]; (c) POPG; and (d) POPG + 150 mM KF. The medium was 50 mM phosphate buffer (pH 7.0). The spectra were recorded at ambient temperature (approx. 20 °C).

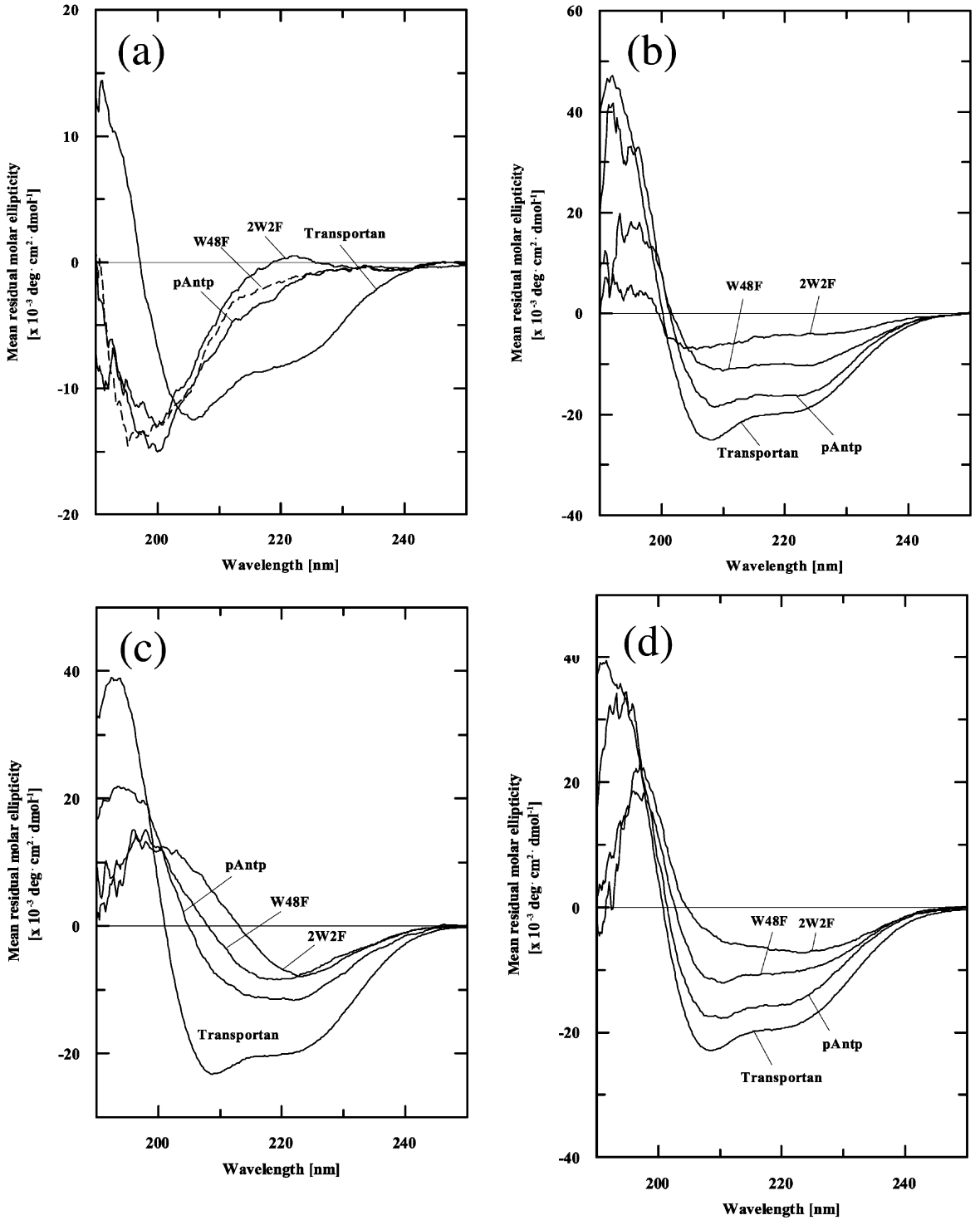
(a)
Mean residual molar ellipticity [x 10⁻³ deg · cm² · dmol⁻¹]
Wavelength [nm]
W48F
2W2F
Transportan
pAntp
(b)
Mean residual molar ellipticity [x 10⁻³ deg · cm² · dmol⁻¹]
Wavelength [nm]
W48F
2W2F
Transportan
pAntp
(c)
Mean residual molar ellipticity [x 10⁻³ deg · cm² · dmol⁻¹]
Wavelength [nm]
pAntp
W48F
2W2F
Transportan
(d)
Mean residual molar ellipticity [x 10⁻³ deg · cm² · dmol⁻¹]
Wavelength [nm]
W48F
2W2F
pAntp
Transportan

Fig. 5.

method applies for a predominating helical structure [20].

4. Discussion

Despite numerous studies on the CPPs, very little is known about their translocation mechanisms in membrane model systems. In recent reports, one group observed pAntp translocation in giant unilamellar vesicles (GUVs) [22], while another group observed that translocation of pAntp does not take place with small or large unilamellar vesicles [23]. It has been suggested that the peptide–lipid interaction is only the first step of a translocation mechanism, which may involve other non-identified protein-mediated transfer processes in cellular systems [24,25]. Whether or not this is the case, the molecular details of the interactions of the CPPs with membrane model systems should provide a valuable basis for understanding the translocation processes.

The present study concerns two types of CPPs, pAntp and transportan, interacting with SUVs of different composition. In order to correlate the behavior with the translocation properties, we have also compared pAntp with two variants (mutants) with different translocating ability in cellular systems, as well as with the CPP pIsl with a single Trp. The pAntp variants are denoted here as W48F and 2W2F, where only the first peptide has a remaining tryptophan residue (Trp56 in pAntp).

Both pAntp and transportan were found to interact with negatively charged membranes, in agreement with previous studies [8]. We have found that at a lipid/peptide molar ratio L/P $\approx$ 100, pAntp is fully bound to POPC/POPG vesicles with surface charge density $\geq$ 20%. Using Trp fluorescence we have established that this is also the case for transportan and W48F (data not shown). Transportan exhibits different behavior. In spite of the net charge of the peptide, the interaction of transportan is mainly charge-independent, requiring only a hydrophobic environment [8]. Thus, the structural changes observed all take place with the peptides fully bound to the vesicles, i.e. the structural changes are not simply due to differing degrees of binding of the peptides to vesicles with different charge density. The CD results (Fig. 5a–d) show that the transportan peptide is mainly helical when bound, and no $\alpha \rightarrow \beta$ transition could be observed when varying the membrane composition or L/P ratio (in the range 12.5–100). This in contrast to the situation with pAntp, where its secondary structure is highly dependent on the surface charge density, as well as on the L/P ratio. An $\alpha \rightarrow \beta$ transition can take place. A high membrane charge, in particular with a low L/P value, promotes a β-structure with pAntp [9]. The 2W2F variant has a lower degree of helicity with vesicles of a low surface charge density (Fig. 5b). On the other hand, 2W2F exhibits a higher degree of β-structure than pAntp at vesicles with a higher surface charge density (Fig. 5c).

From the effect of the non-charged quencher acrylamide, we can observe that for pAntp, as well as its variant, W48F, there is no interaction with neural (POPC) vesicles (Table 1; Fig. 2 a,b). With negatively charged vesicles of 30% and 100% surface charge density, the peptides exhibit almost the same quenching constants and wavelength of the Trp fluorescence maximum, indicating the same nature of interaction. However, the accessibility of the Trp residues of pAntp to the quencher also appears to be affected by the lipid/peptide molar ratio (L/P). At low L/P, where a dominating β-structure is observed for pAntp, the Trp residues are less accessible to the quencher (Table 1).

A similar trend is observed with the quenching effect of free spin-labeled fatty acids (Table 2; Fig. 3a,b). At the highest surface-charge density (100% POPG), there is a considerable reduction in the quenching constants with pAntp and W48F, indicating that the Trp residues are more hidden from the quenchers at vesicles composed of pure POPG than with only 30% POPG. The results

Fig. 5. CD spectra of 10 μM peptides in the presence of different media: (a) buffer; (b) 1 mM POPG/POPC [30:70] vesicles; (c) 1 mM POPG vesicles; and (d) 1 mM POPG vesicles with 150 mM KF added to the buffer. The medium used was 50 mM phosphate buffer (pH 7.0) and the temperature was set at 20 °C.

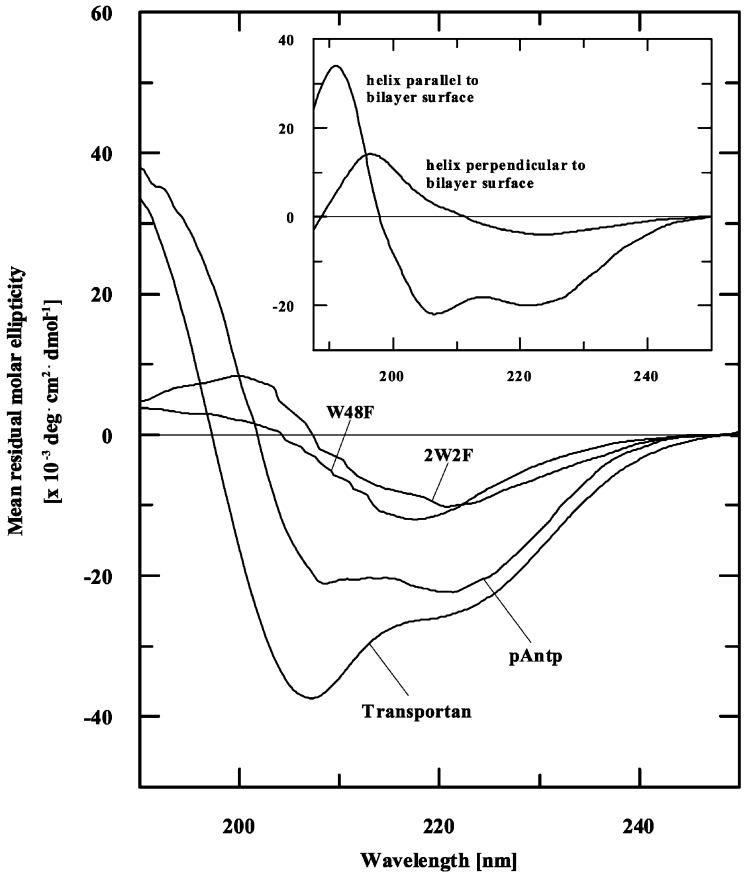

Fig. 6. Oriented CD (OCD) spectra of pAntp and its two variants, W48F and 2W2F, in the presence of oriented POPG/POPC [30:70] multibilayers, at an L/P ratio of 100. The spectra were recorded with the membrane surface oriented perpendicular to the optical axis. The temperature was set at 20 °C. Insert: the OCD spectra of helices in the two extreme orientations, after Wu et al. [20].

with different quenchers suggest an aggregation of pAntp at high vesicle surface-charge density and low L/P, which makes the Trp residues within a β-state less accessible to any quencher.

This picture is different for transportan. From an earlier study we know that the interaction of transportan is not dependent on the charge of the bilayer, with no difference observed by the acrylamide quenching for neutral (POPC) and fully charged (POPG) vesicles [8]. From the spin-labeled fatty acid quenching experiments (Table 2; Fig. 3a,b), we can observe that in this case there is also no further significant reduction in the quenching constant at the highest surface-charge density.

In terms of the membrane perturbation (order) as revealed by the DPH polarization, again we observe differences between the two CPPs, penetratin and transportan. In the case of pAntp there is a structure-dependent membrane effect. With POPG/POPC [30:70] vesicles, pAntp does not significantly affect the DPH polarization (Fig. 4b). This shows that pAntp does not perturb the membrane order when the peptide is bound with an α-helical conformation (Fig. 5b). This is supported by an earlier ^{31}P-NMR study, which report-

ed that pAntp interacts with phospholipid vesicles of approximately 20% charge density, without changing the bilayer organization [26]. With 100% charged vesicles the situation is quite different, and here a strong perturbation of the membrane order is observed (Fig. 4c). pAntp then adopts a more β-like conformation, possibly in an aggregated form (Fig. 5c). Screening the effect of electrostatics by adding salt (150 mM KF) shifts the structure towards a more helical structure, with a corresponding reduction in the membrane perturbation (Fig. 4d and Fig. 5d). The 2W2F variant always perturbs the membrane to a greater extent than pAntp, at all lipid charge density values (Fig. 4a–d).

Transportan induces the same of degree of increase in DPH polarization, regardless of the lipid charge density (Fig. 4a–d). The almost constant increase in the DPH polarization is probably due to higher ordering in the membrane caused by similar interaction of a transportan moiety, resulting in a similar degree of perturbation, regardless of the lipid charge density. Since DPH is buried deeply within the acyl region of the bilayer, an increase in the polarization should report on decreased acyl-chain mobility and increased chain order in the hydrophobic core [27]. The increase in DPH polarization is to be expected for a hydrophobic peptide such as transportan. Such changes have also been observed with the insertion of other hydrophobic peptides into a membrane [28].

An increase in the DPH polarization anisotropy due to peptide aggregation has been reported for the β-amyloid peptide (Aβ) [29,30], as well as for the functional variant OmpA signal peptides [31]. With the Aβ, the aggregated form of the peptide was found to increase DPH anisotropy as opposed to the unaggregated form, which had no effect. Based on our results, it is possible that pAntp behaves similarly.

The lack of distinction of fluorescence behavior between the two Trp residues of pAntp indicates that they reside in the same region within the vesicles. This suggests that pAntp lies flat, parallel to the bilayer near the surface. This is supported by our OCD experiments, in which conditions were chosen to secure tight binding with a preferentially α-helical structure. The spectrum for pAntp (Fig. 6) is characteristic of a helix lying perpendicular to the bilayer normal, i.e. parallel to the bilayer surface [20,21]. Transportan also appears to be oriented parallel to the bilayer surface, although a difference from the pAntp OCD spectrum is observed (Fig. 6). It is possible that this difference is due to spectral distortions caused by considerable random-coil contributions. Alternatively, it could be due to a small tilt angle resulting from the highly hydrophobic mastoparan component of transportan. Similarly, mastoparan has recently been studied by NMR in a bicellar solvent, and was shown to lie perpendicular to the bilayer normal in zwitterionic bicelles, while in anionic bicelles it inserts parallel to the bilayer normal [32]. The OCD spectra for the two pAntp variants are quite different. Assuming that they are helical, they may insert more parallel to the bilayer normal (i.e. perpendicular to the bilayer surface). This unexpected difference may be related to the different membrane translocation abilities.

A study of phospholipid monolayers with surface infrared (IR) spectroscopy has suggested that pAntp is preferentially adsorbed onto charged phospholipids parallel to the surface [33]. Recently, neutron reflectivity was applied in order to locate the pAntp molecule with phospholipid deposits [34]. The low resolution only allowed localization of peptide particles near the headgroup region of the membrane. Molecular modeling calculations indicate that pAntp remains at the surface of the vesicle [23]. This is to be expected, since it has generally been found that cationic peptides initially bind at the interface perpendicular to the bilayer normal [35].

We have estimated the position of the Trp residues of the peptides relative to the center of the bilayer, applying the parallax fluorescence method [15]. As for the OCD studies, sample conditions favoring an α-helical bound state were employed. The values obtained (Table 3) indicate that the Trp residues of the peptides studied are all close to the surface, just below the headgroups. This is in agreement with the results with acrylamide and spin-labeled fatty-acid quencher.

The Trp48 residue is conserved between all the homeodomains, including Isl-1 [36]. Trp residues have also been suggested to be crucial for the translocation of homeodomains and derived CCPs [37]. In the case of 2W2F, where both Trp residues have been replaced by phenylalanine, the translocation ability has been completely abolished [3]. It has been reported [11] that the translocation ability of pAntp and variants is more affected by truncations and modifications in the C-terminal segment, compared to the N-terminus. It has been suggested that the Trp48 residue of pAntp acts as an anchor to the surface of the bilayer [4]. In the model proposed for the translocation mechanism, the whole process begins with destabilization of the lipid bilayer by Trp48. The concept of an anchor residue appears not to be restricted to CPPs; it has even been suggested for antimicrobial peptides. In a study on a synthetic antimicrobial peptide chimera (cecropin–magainin), it was proposed that a Trp residue functions as an anchor, playing a role in the primary binding of the peptide to the membrane [38].

With transportan, it has been shown that a segment in which six residues at the N-terminus have been deleted still translocates [39]. In this shorter peptide there is no Trp residue. This means that the necessity of a Trp anchor does not apply to transportan, and perhaps the whole or part of its N-terminal sequence, derived from galanin, fulfills the role of an anchor (cf. Öhman et al. [40], who showed that the full galanin peptide is located very close to the surface of an SDS micelle).

It is between pAntp and its non-translocating variant, 2W2F, that several significant differences are observed in the membrane interaction characteristics. 2W2F, with no translocating ability, is more hydrophobic than pAntp, and may insert more deeply into the bilayer, more parallel to the bilayer normal according to the OCD result. This would explain the greater degree of membrane perturbation. pAntp, on the other hand, appears to lie perpendicular to the bilayer normal (along the surface), probably anchored by its Trp48 just below the headgroups, until such conditions are created that the translocation transiently can take place. This metastable positioning of the pAntp peptide in the charged membrane may be crucial for the bilayer destabilization and the translocating properties.

Penetratin and transportan can be considered as being two types within the CPP family, not necessarily following the same translocation phenomenon in detail. Whether any secondary structure is involved in the transient permeation of a CPP is still an open question. There is no evidence for the formation of any defined oligomeric structures, such as pores, within the membrane. Such a state will hardly be compatible with the great diversity in the nature and size of the ‘cargo’ which the CPPs is able to pull through a cell membrane, with the mechanisms still being some kind of mystery and a biophysical challenge.

Acknowledgments

This study was supported by grants from the Swedish Science Council and from the EU Program Contract No MAS3-CT97-0156.

References

[1] D. Derossi, G. Chassaing, A. Prochiantz, Trojan peptides: the penetratin system for intracellular delivery, Trends Cell Biol. 8 (1998) 84–87.
[2] M. Lindgren, M. Hällbrink, A. Prochiantz, Ü. Langel, Cell-penetrating peptides, Trends Pharmacol. Sci. 21 (2000) 99–103.
[3] D. Derossi, A.H. Joliot, G. Chassaing, A. Prochiantz, The third helix of Antennapedia homeodomain translocates through biological membranes, J. Biol. Chem. 269 (1994) 10444–10450.
[4] D. Derossi, S. Calvet, A. Trembleau, A. Brunissen, G. Chassaing, A. Prochiantz, Cell internalization of the third helix of the Antennapedia homeodomain is receptor-independent, J. Biol. Chem. 271 (1996) 18188–18193.
[5] A. Prochiantz, Homeodomain-derived peptides in and out of the cells, Ann. NY Acad. Sci. 886 (1999) 172–179.
[6] I. Le Roux, A.H. Joliot, E. Bloch-Gallego, A. Prochiantz, M. Volovitch, Neurotrophic activity of the Antennapedia homeodomain depends on its specific DNA-binding properties, Proc. Natl. Acad. Sci. USA 90 (1993) 9120–9124.
[7] K. Kilk, M. Magzoub, M. Pooga, G. Eriksson, Ü. Langel, A. Gräslund, Cellular internalization of a cargo complex with a novel peptide derived from the third helix of the islet-1 homeodomain. Comparison with the

penetratin peptide, Bioconjugate Chem. 12 (2001) 911–916.
[8] M. Magzoub, K. Kilk, L.E.G. Eriksson, Ü. Langel, A. Gräslund, Interaction and structure induction of cell-penetrating peptides in the presence of phospholipid vesicles, Biochim. Biophys. Acta 1516 (2001) 77–89.
[9] M. Magzoub, L.E.G. Eriksson, A. Gräslund, Conformational states of the cell-penetrating peptide penetratin when interacting with phospholipid vesicles: effects of surface charge and peptide concentration, Biochim. Biophys. Acta, 1563 (2002) 53–63.
[10] M. Pooga, M. Hällbrink, M. Zorko, Ü. Langel, Cell penetration by transportan, FASEB J. 12 (1998) 67–77.
[11] P.M. Fischer, N.Z. Zhelev, S. Wang, J.E. Melville, R. Fåhraeus, D.P. Lane, Structure–activity relationship of truncated and substituted analogues of the intracellular delivery vector penetratin, J. Peptide Res. 55 (2000) 163–172.
[12] G. Drin, M. Mazel, P. Clair, D. Mathieu, M. Kaczorek, J. Temsamani, Physico-chemical requirements for cellular uptake of pAntp peptide. Role of lipid-binding affinity, Eur. J. Biochem. 268 (2001) 1304–1314.
[13] B.-M. Backlund, G. Wikander, T. Peeters, A. Gräslund, Induction of secondary structure in the peptide hormone motilin by interaction with phospholipid vesicles, Biochim. Biophys. Acta 1190 (1994) 337–344.
[14] J.R. Lakowicz, Principles of Fluorescence Spectroscopy, 2nd ed., Kluwer Academic, New York, 1999.
[15] A. Chattopadhyay, E. London, Parallax method for direct measurement of membrane penetration depth utilizing fluorescence quenching by spin-labeled phospholipids, Biochemistry 26 (1987) 39–45.
[16] F.S. Abrams, E. London, Analysis of protein and peptide penetration into membranes by depth-dependent fluorescence quenching: theoretical considerations, Biochemistry 32 (1993) 10826–10831.
[17] P. Manavalan, W.C. Johnson Jr, Variable selection method improves the prediction of protein secondary structure from circular dichroism spectra, Anal. Biochem. 167 (1987) 76–85.
[18] G.A. Olah, H.W. Huang, Circular dichroism of oriented helices. I. Proof of the exciton theory, J. Chem. Phys. 89 (1988) 2531–2538.
[19] G.A. Olah, H.W. Huang, Circular dichroism of oriented helices. II. Electric field-oriented polypeptides, J. Chem. Phys. 89 (1988) 6956–6962.
[20] Y. Wu, H.W. Huang, G.A. Olah, Method of oriented circular dichroism, Biophys. J. 57 (1990) 797–806.
[21] W.C. Wimley, S.H. White, Designing transmembrane alpha-helices that insert spontaneously, Biochemistry 39 (2000) 4432–4442.
[22] P. Thorén, D. Persson, M. Karlsson, B. Nordén, The Antennapedia peptide penetratin translocates across lipid bilayers—the first direct observation, FEBS Lett. 482 (2000) 265–268.
[23] G. Drin, H. Déméné, J. Temsamani, R. Brasseur, Translocation of the pAntp peptide and its amphipathic analogue AP-2AL, Biochemistry 40 (2001) 1824–1834.
[24] A. Scheller, J. Oehlke, B. Wiesner, et al., Structural requirements for cellular uptake of α-helical amphipathic peptides, J. Peptide Sci. 5 (1999) 185–194.
[25] J. Oehlke, A. Scheller, B. Wiesner, et al., Cellular uptake of an α-helical amphipathic model peptide with the potential to deliver polar compounds into the cell interior non-endocytically, Biochim. Biophys. Acta 1414 (1998) 127–139.
[26] J.-P. Berlose, O. Convert, D. Derossi, A. Brunissen, G. Chassaing, Conformational and associative behaviours of the third helix of Antennapedia homeodomain in membrane-mimetic environments, Eur. J. Biochem. 242 (1996) 372–386.
[27] B.R. Lentz, Use of fluorescent probes to monitor molecular order and motions within liposome bilayers, Chem. Phys. Lipids 64 (1993) 99–116.
[28] J.M. Mancheno, M. Gasset, J.P. Albar, et al., Membrane interaction of a beta-structure-forming synthetic peptide comprising the 116–139th sequence region of the cytotoxic protein alpha-sarcin, Biophys. J. 68 (1995) 2387–2395.
[29] J.J. Kremer, M.M. Pallitto, D.J. Sklansky, R.M. Murphy, Correlation of β-amyloid aggregate size and hydrophobicity with decreased bilayer fluidity of model membranes, Biochemistry 39 (2000) 10309–10318.
[30] J.J. Kremer, D.J. Sklansky, R.M. Murphy, Profile of changes in lipid bilayer structure caused by β-amyloid peptide, Biochemistry 41 (2001) 8563–8571.
[31] D.W. Hoyt, L.M. Gierasch, Hydrophobic content and lipid interactions of wild-type and mutant OmpA signal peptides correlate with their in vivo function, Biochemistry 30 (1991) 10155–10163.
[32] J.A. Whiles, R. Brasseur, K.J. Glover, G. Melacini, E.A. Komives, R.R. Vold, Orientation and effects of mastoparan X on phospholipid bicelles, Biophys. J. 80 (2001) 280–293.
[33] E. Bellet-Amalric, D. Blaudez, B. Desbat, F. Graner, F. Gauthier, A. Renault, Interaction of the third helix of Antennapedia homeodomain and a phospholipid monolayer, studied by ellipsometry and PM-IRRAS at the air–water interface, Biochim. Biophys. Acta 1467 (2000) 131–143.
[34] G. Fragneto, F. Graner, T. Charitat, P. Dubos, E. Bellet-Amalric, Interaction of the third helix of Antennapedia homeodomain with a deposited phospholipid bilayer: a neutron reflectivity structural study, Langmuir 16 (2000) 4581–4588.
[35] L. Zhang, A. Rozek, R.E.W. Hancock, Interaction of cationic antimicrobial peptides with model membranes, J. Biol. Chem. 276 (2001) 35714–35722.
[36] O. Karlsson, S. Thor, T. Norberg, H. Ohlsson, T. Edlund, Insulin gene enhancer binding protein Isl-1 is a member

of a novel class of proteins containing both a homeo- and a Cys–His domain, Nature 344 (1990) 879–882.
[37] A. Prochiantz, Getting hydrophilic compounds into cells: lessons from homeopeptides, Curr. Opin. Neurobiol. 6 (1996) 629–634.
[38] D. Oh, S.Y. Shin, S. Lee, et al., Role of the hinge region and the tryptophan residue in the synthetic antimicrobial peptides, cecropin A(1–8)-magainin 2(1–12) and its analogues, on their antibiotic activities and structures, Biochemistry 39 (2000) 11855–11864.
[39] U. Soomets, M. Lindgren, X. Gallet, et al., Deletion analogues of transportan, Biochim. Biophys. Acta 1467 (2000) 165–176.
[40] A. Öhman, P.-O. Lycksell, A. Juréus, Ü. Langel, T. Bartfai, A. Gräslund, NMR study of the conformation and localization of porcine galanin in SDS micelles. Comparison with an inactive analog and a galanin receptor antagonist, Biochemistry 37 (1998) 9169–9178.